URN (Paper): urn:nbn:de:gbv:ilm1-2014iwk-059:9
58th ILMENAU SCIENTIFIC COLLOQUIUM
Technische Universität Ilmenau, 08 – 12 September 2014
URN: urn:nbn:de:gbv:ilm1-2014iwk:3

STABILITY OF A FULLY FIBRE-COUPLED INTERFEROMETER

Christoph Weichert[1], Paul Köchert[1], Rainer Köning[1], Jens Flügge[1]*

[1]Physikalisch-Technische Bundesanstalt, Bundesallee 100, D-38116 Braunschweig, Germany

ABSTRACT

The long-time stability of interferometer can be increased by separating heat sources using optical fibres. But the use of multimode fibres to transfer the superposed beams to the detectors can also increase the measured phase variations. A Mach-Zehnder setup, which represents a minimized realization of a heterodyne interferometer with spatially separated input beams, was used to analyse the noise limitations of interferometer and the influence of multimode fibres. The resolution was measured and calculated for different beat frequencies and receivers. According to the used beat frequency the noise is dominated by either the shot noise and amplifier noise or the laser intensity noise. The minimal standard deviation of 4.8 pm over 60 s was achieved both with and without the use of fibres. In case of long-time measurements the position variations were observed to be ±20 pm, which were introduced by the fibres. Their disturbing influence was increased by stimulating mode conversion.

Index Terms **–** heterodyne interferometer, long-time stability, multimode fibres

1. INTRODUCTION

The inherent traceability of optical interferometers makes them an ideal choice for high accuracy differential length measurements. In order to meet the rising demands of industry and international projects, like the Avogadro project, the uncertainty of length measurements has to decrease continuously and needs to be in the sub-nanometre range. Therefore, the PTB developed an adaptable phase meter based on an ADC-FPGA board [1]. In case the phase meter was fed with signals of a function generator, the phase exhibited a standard deviation below 35 µrad at an acquisition rate of 48.8 kHz. This corresponds to a variation of the position of 1.5 pm at a single path interferometer working with light with a wavelength of 532 nm. Additionally the PTB realised heterodyne interferometers using spatially separated input beams to avoid periodic nonlinearities. The NIST has shown that this design principle is suitable to reduce the periodic nonlinearities to the picometre regime [2]. It was shown by comparing an optical interferometer and an x-ray interferometer that the periodic nonlinearities can be below ±10 pm [3]. Due to the reduced contribution of the nonlinearities the uncertainty of interferometer setups with a negligible death path used for measurements in the millimetre range or of interferometer setups working in a vacuum environment is limited by other error sources. There is a gain of importance concerning the detection noise, amplitude noise of the light source and the long-time stability of the setup. For a heterodyne interferometer with spatially separated input beams and a negligible dead path PTB had measured a phase variation correlated to a temperature variation of approximately 120 mrad/K [4], corresponding to 5 nm/K for a single path interferometer. Other interferometer systems show temperature dependent variations of the same magnitude. Examples are the Zygo "Differential plane mirror interferometer" specified with 10 nm/K (400 mrad/K), the Agilent 10716A specified with 40 nm/K (1.589 rad/K) and depending on the material combination between 0.3 nm/K and 2 nm/K (12 – 79 mrad/K) achieved by Hosoe for a double-path interferometer [5]. The thermal drift of an interferometer may be caused by many reasons like asymmetric optical components and mounts, an asymmetric fixing of the holder, asymmetric thermal expansion of the materials and temperature gradients. Consequently, a drift is hard to avoid and for an improvement of the long-time stability it is necessary to improve the thermal stability. This can be realized by avoiding heat sources close to the optical setup by using optical fibres.

The desired, fully fibre-coupled configuration also affects the stability of the interferometer setup. The influence of polarisation-maintaining fibres on the uncertainty of a fibre-feed heterodyne interferometer is discussed in several publications. The importance of the polarisers behind the fibres to reduce the influence of the second guided mode is described in [6] and [7]. For the work in the sub-nanometre range also the recycled light from angle polished fibres used to transfer the light to the setup affects the noise of the interferometers as it is described by Mana [8]. In this publication, we analyse the influence of different multimode fibres used to transfer the superposed beams to the detectors. We performed these investigations using a Mach-Zehnder setup to minimize the impact of other components. To separate the effects caused by the fibres from the detection noise we have analysed the noise of the interferometer setup before.

2. MACH ZEHNDER SETUP

A Mach-Zehnder setup is a simple realisation of an interferometer. It contains the minimal number of parts of a heterodyne interferometer with spatially separated input beams. Therefore it is suitable to analyse the influence of the different components on the measured phase variation without disturbing effects of the interferometer optics or a mirror movement. The results presented in this contribution were achieved using the Mach-Zehnder setup shown in figure 1. A frequency-doubled Nd:YAG laser operating at 532 nm was used as light source. Its emitted light passed through an optical isolator and was split using a half wave plate and a polarisation beam splitter (PBS). This configuration allows to adjust the amount of light used

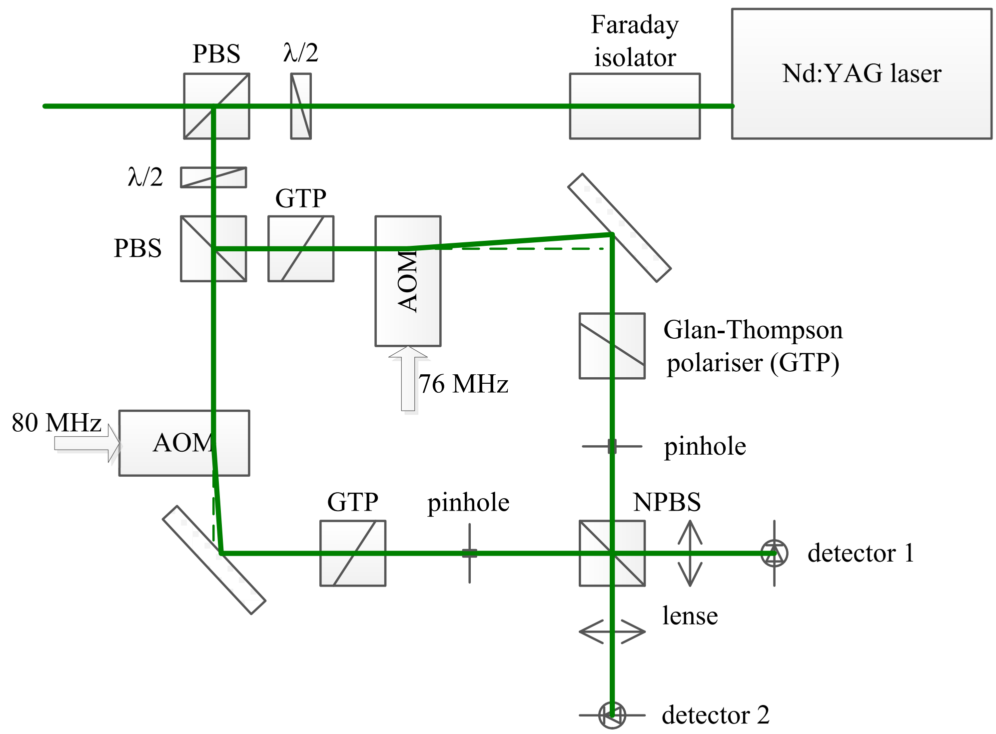

Figure 1: Arrangement of the components of the Mach-Zehnder setup

for the Mach-Zehnder interferometer. Another half wave plate and polarisation beam splitter were used to split the light again. The part of the light reflected at the PBS passed through a Glan-Thompson polariser (GTP) which removes the leaked part of the parallel polarised light. After this the light passed through an acousto-optical modulator (AOM), which shifted its frequency by 76 MHz. The part of the light transmitted at the PBS passed through another half wave plate used to adapt its polarisation state and afterwards through an acousto-optical modulator, which shifted its frequency by 80 MHz. The polarisation state of each frequency shifted beam was filtered again using two Glan-Thompson polarisers before they were superposed at a non-polarising beam splitter (NPBS). These polarisers have to be aligned to the same angle to avoid disturbing effects. These disturbances are caused by the polarisation depended reflectivity of the non-polarising beam splitter in combination with a possible variation of the phase difference between both polarisation states, as shown in [6] and [7]. The two recombined beams were focused on detectors resulting in two signals with a frequency of 4 MHz. Due to the principle of conservation of energy, the two detected signals should exhibit a constant phase difference of π. However, the detected phase difference varies because of the different noise sources. Therefore, this phase variation was used to analyse the limitations of heterodyne interferometer with regard to the resolution and the stability.

3. NOISE LIMITATION

The resolving capability of heterodyne interferometer is particularly limited by the detection noise. We will develop a simple theoretical model, which estimates the resolution limitations caused by the amplitude noise. The displacement (s) of a plane-mirror interferometer is calculated according to equation (1), with the usage of the measured phase difference (φ) and the wavelength of the light source (λ):

$$\begin{aligned} s &= \frac{\lambda}{4\,\pi}\,\varphi \\ &= \frac{\lambda}{4\,\pi}\,(\varphi_1 - \varphi_2) \end{aligned} \tag{1}$$

For the following considerations the wavelength is assumed to be constant. The phase determination is based on the phase meter [1] working with a digital lock-in algorithm. The signals (s_1 and s_2) are multiplied each with a sine and cosine reference waveform and perform a low-pass filtering using a preassigned window function. With the resulting two values for each channel ($s_{i\,S}$ and $s_{i\,C}$) the fraction of the optical fringe is calculated using the inverse tangent function. This calculated phase value (φ_i) depends on the relative delay of the synthetic internal reference to the signal. But this arbitrary phase is the same for both signals and is removed by calculating the difference of both phase values. The standard uncertainty of the measured phase (φ) can be determined using the law of error propagation. It contains the variances of the signals, their correlation coefficient and the corresponding partial derivatives [9].

$$u_s = \frac{\lambda}{4\,\pi}\sqrt{u_{\varphi_1}^2 + u_{\varphi_2}^2 - 2\,r\,u_{\varphi_1}u_{\varphi_2}} \tag{2}$$

Because the signals are acquired by similar detectors and analogue-digital converters (ADC), their variances are assumed to be equal ($u_{\varphi_1}^2 = u_{\varphi_2}^2 = u^2$). The phase noise is related to the amplitude noise [2].

$$|\Delta\varphi| = \left|\frac{\Delta R}{R}\right| \tag{3}$$

The amplitude deviations result from the variance of the photo current multiplied with a factor. This factor depends on the amplification of the transimpedance amplifiers and the bandwidth (B) of the phase evaluation derived from the window function. This factor is the same for the temporal average of the signal current. Therefore the signal-to-noise ratio of the amplitude is the same for the currents.

$$|\Delta\varphi| = \left|\frac{\Delta R}{R}\right| = \frac{\langle \Delta i^2 \rangle}{\langle i_{\mathrm{signal}}^2 \rangle} \tag{4}$$

The amplitude of the signal current at the beat frequency is given by the sensitivity of the photo diode (S), the light power (P_0) and the interference contrast (m). The temporal average of the quadratic signal current (i_{signal}^2) can be determined with the equation (5).

$$\langle i_{\mathrm{signal}}^2 \rangle = 0.5 \cdot (m\, S\, P_0)^2 \tag{5}$$

The amplitude variations of the signal current are caused by the shot noise, the noise of the amplifiers, the noise of ADC and the intensity noise of the laser. The shot noise is calculated according to equation (6) We neglect the contribution of the dark current of the photo diode, because it is insignificant here.

$$\langle \Delta i_{\mathrm{Shot}}^2 \rangle = 2\, q\, S\, P_0\, B \tag{6}$$

In this setup custom-made photo receivers by FEMTO GmbH, which consist of a photo diode and a transimpedance amplifier, were used. Their noise is specified by a measured noise equivalent power (NEP). The manufacturer's specifications are listed in table 1. With the sensitivity of the photo diode at 532 nm and the bandwidth of the phase evaluation algorithm an adequate current variance can be calculated.

$$\langle \Delta i_{\mathrm{NEP}}^2 \rangle = (S \cdot NEP)^2\, B \tag{7}$$

In the same way the noise of the ADCs can be transferred to an adequate current variance at the input of the transimpedance amplifier. For this purpose the size of the feedback resistor (R_f) of the amplifiers (its magnitude equals the amplification) is required. The manufacturer of the ADC/FPGA board (Struck Innovative Systeme GmbH) specifies the scatter of the 16-bit ADCs with a standard deviation of 2.7 digits measured at 100 MHz with a terminated input. The model of this noise contribution is provided by equation (8). It was observed that already far below the limits of the input range 3.2 V of the ADCs their nonlinear deviations like the integral and differential nonlinearities occur. Those were accompanied by an increase of the amplitude noise, which is obviously not included in equation (8).

$$\langle \Delta i_{\mathrm{ADC}}^2 \rangle = \left(\frac{2.7}{65536}\, \frac{3.2\ \mathrm{V}}{R_f}\right)^2 \cdot \frac{B}{100\ \mathrm{MHz}} \tag{8}$$

A variation of the laser power close to the beat frequency within the bandwidth of the phase evaluation algorithm cannot be distinguished from a phase variation. For the Prometheus laser of Coherent a relative intensity noise (RIN) of -150 dB/Hz is specified at a frequency of 4 MHz. This value can be converted in a variance of the current [10] using equation (9).

$$\langle \Delta i_{\mathrm{RIN}}^2 \rangle = \left(S\, P_0\, 10^{RIN/20}\right)^2 B \tag{9}$$

Naturally, the light of laser is used for both receivers. Therefore, the intensity noise affects both signals, but due to the phase shift of π in opposite directions. The related correlation coefficient can be calculated by the equation (10) according to [9], if the noise of the two receivers and ADCs are assumed to be uncorrelated.

$$r = -\frac{\langle \Delta i_{\text{RIN}}^2 \rangle}{\langle \Delta i_{\text{Shot}}^2 \rangle + \langle \Delta i_{\text{NEP}}^2 \rangle + \langle \Delta i_{\text{ADC}}^2 \rangle + \langle \Delta i_{\text{RIN}}^2 \rangle} \tag{10}$$

Using equations (4) to (10) equation (2) can be transferred to equation (11).

$$u_s = \frac{\lambda}{4\,\pi} \sqrt{\frac{2\,\langle \Delta i_{\text{Shot}}^2 \rangle + 2\,\langle \Delta i_{\text{NEP}}^2 \rangle + 2\,\langle \Delta i_{\text{ADC}}^2 \rangle + 4\,\langle \Delta i_{\text{RIN}}^2 \rangle}{0.5 \cdot (m\,S\,P_0)^2}} \tag{11}$$

The amplitude noise limit of heterodyne interferometers can be estimated using equation (11). The specifications and the calculated noise for three different receivers used in this investigation are listed in table 1. All values are below 15 pm (354 µrad). The dominating contributions are caused by the shot noise and the specific noise of each receiver. But this finding changes completely for a beat frequency of 1.5 MHz. Here the relative intensity noise of the laser is -135 dB/Hz, so that the contribution of the laser becomes the dominant noise source. We like to note here that the noise analysis provided still misses some contributions, which are difficult to quantify. For example an additional analysis of the phase meter using a frequency generator had shown that the noise of the phase meter correlates with the beat frequency. In addition, the signal-to-noise ratio of the ADCs depends on the jitter contribution of the clock signal. The smaller the beat frequency the smaller is the influence of the clock jitter.

The phase variations were also measured at the Mach-Zehnder setup using these three different amplifiers. We measured the phase variations over several minutes with an acquisition rate of 48.8 kHz. The mean standard deviation of the measured phase values over 60 seconds (2929688 phase values) are also listed in table 1 for the three different receivers. The measured standard deviations have similar magnitudes as the calculated noise, but the calculation cannot be fully confirmed. This may be caused by large number of simplifications used. The calculation still neglects all nonlinear behaviour of the amplifiers and ADCs as well as electrical crosstalk at the phase meter. Further it was assumed, that the power of the light

Receiver	1	2	3
Measured standard deviation (60s) at beat frequency of 4 MHz	4.9 pm	9.9 pm	7.8 pm
Calculated noise for 4 MHz	6.5 pm	11.6 pm	6.8 pm
Upper cut-off frequency	10 MHz	40 MHz	100 MHz
Optical power P_0	65 µW	45 µW	85 µW
feedback resistor R_f	73 kΩ	100 kΩ	50 kΩ
NEP of the amplifier at 850 nm and 4 MHz	3.8 pW/$\sqrt{\text{Hz}}$	6.0 pW/$\sqrt{\text{Hz}}$	6.0 pW/$\sqrt{\text{Hz}}$
Sensitivity (S) at 532 nm	0.28 A/W		
Interference contrast (m)	0.75		
Bandwidth algorithm (B)	90 kHz		
RIN laser at 4 MHz	-150 dB/Hz		
Calculated shot noise	4.5 pm	5.4 pm	3.9 pm
Calculated noise for 1.5 MHz (RIN = -135 dB/Hz)	10.6 pm	14.3 pm	10.8 pm
Measured standard deviation (60s) at beat frequency of 1.5 MHz	11.3 pm	13.1 pm	12.5 pm

Table 1: Noise at the Mach-Zehnder setup for three different amplifiers, measured (blue rows) and calculated (yellow rows)

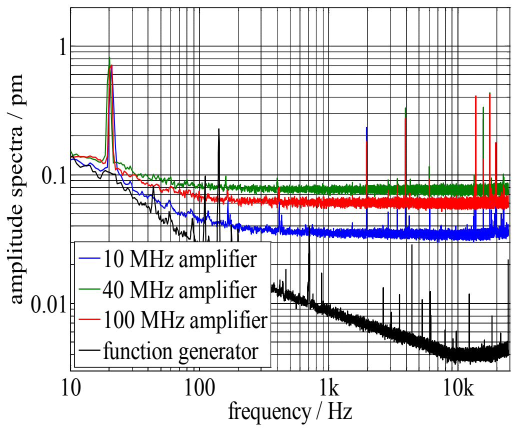

Figure 2(a): beat frequency of 4 MHz

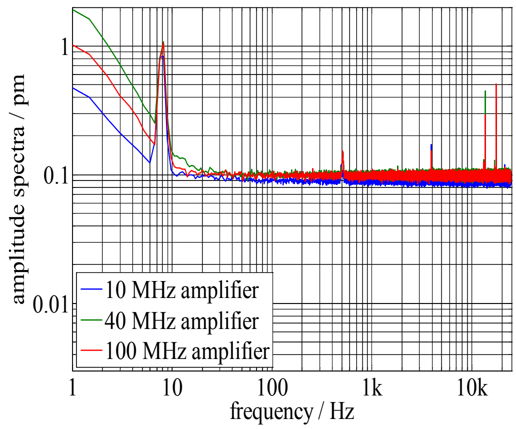

Figure 2(b): beat frequency of 1.5 MHz

Figure 2:amplitude spectra of the phase variations measured at the Mach-Zehnder setup with an acquisition rate of 48.8 kHz with different amplifiers

and the contrast was equal at both photo detectors. However, the non-polarising beam splitter does not split the light in equal parts. Furthermore, the same power supply was used for both receivers, therefore their noise may also be correlated. Additionally, it was recognized that a thermalisation time of at least one hour is required for the amplifiers. Otherwise phase variations resulting from thermalisation effects were observed, see figure 3.

The amplitude spectra of the measured phase variation are shown in figure 2 for the three amplifiers. The differences observed between the different beat frequencies are clarified in a comparison of the figure 2(a) and 2(b). At a beat frequency of 4 MHz, a different noise floor is observable for the three amplifiers, because the position noise is dominated by shot and amplifier noise. At a beat frequency of 1.5 MHz the intensity noise of the laser, whose influence is independent of the amplification and light power, is dominating and therefore the noise floor is similar for the three amplifiers. At both beat frequencies the amplitude spectra exhibit a peak below 30 Hz. These peaks (21 Hz at 4 MHz and 8 Hz at 1.5 MHz) are caused by the phase evaluation itself. Using a clock synchronisation between the phase meter electronics and the function generator, supplying the signal for the AOMs, or using a different acquisition rate would avoid these peaks.

4. INFLUENCE OF MULTIMODE FIBRES AT THE INTERFEROMETER OUTPUT

In a second step we placed multimode fibres between the non-polarising beam splitter and the receivers, see figure 1. We measured the phase variations with the receivers of type 1 (10 MHz bandwidth). These measurements were repeated for three different types of multimode fibres. The fibres were exchanged pairwise to analyse of the influence of core diameter. All tested fibres had a length of 5 m and a numerical aperture (NA) of 0.22 and they were angle polished. The parameters of the used fibres and the measurement results are listed in table 2. The observed phase variations over a time of 60 s are similar to the ones measured before without the fibres had been integrated at the setup. This holds for any fibre. For the measurements with fibres the phase variations observed over several hours were larger than those without fibres. Figure 3 shows the phase variations measured at the Mach-Zehnder setup over 10 hours both with and without the use of multimode fibres. At an acquisition rate of 1 kHz a standard deviation of 3.0 pm was determined without fibres and a standard deviation of 11.7 pm with step index fibres with a core diameter of 300 µm. During these measurements the fibres and the two receivers were placed on the same breadboard as the

Fibre	1	2	3
Measured standard deviation (60s) at beat frequency of 4 MHz	4.8 pm	5.2 pm	4.8 pm
Measured standard deviation without fibres	4.8 pm		
Fibre type	step index	gradient index	step index
Core diameter	50 µm	62.5 µm	300 µm
Measured standard deviation (60s) with disturbance source	6.0 pm	9.5 pm	11.3 pm

Table 2: Influence of multimode fibres obtained by measurements

entire Mach-Zehnder setup in a temperature controlled laboratory in the basement of the building. Without fibres the mean phase varied in the range of ±5 pm, due to the temperature-dependent delay of the amplifiers. While using multimode fibres the mean phase varied in the range ±20 pm. This increased phase variation may be caused by mode conversion. Multimode fibres with such a large core diameter guide a very large number of modes and each mode propagates with a specific velocity. Therefore, a variation of the mode distribution will cause an alternating signal delay, which in turn causes a phase variation. An exact and adequate calculation is rather complicated. Therefore, the maximal magnitude of the influence is estimated with the crude approximation of the maximum delay time for weak guiding step fibres given in equation (12).

$$\Delta T_{\mathrm{max}} = \frac{NA^2\, L}{2\, n_{\mathrm{core}}\, c} \tag{12}$$

To use the equation (12), which is obtained from [11], the speed of light in vacuum (c), the refractive index of the core ($n_{\mathrm{core}} = 1.5$) and the length of the fibre (L) is required. The maximum possible delay is converted to a position variation in picometre and amounts for the used step index fibres to 280 pm, which demonstrates that a more detailed analysis is required.

Additionally, the fibres were directly attached to the photo diodes and it was not possible to verify whether the beam diameter was smaller than the diameter of the active area of the photo diode. If the beam diameter was larger, the effect of the mode conversion would be increased due to the related change of the intensity pattern hitting the detector surface.

The mode conversion was also stimulated by placing one of the two multimode fibres in use onto another table and attaching a speaker to it. The speaker was operated with a sinusoidal waveform with a frequency of 500 Hz. The change of the amplitude spectra of the measured phase is illustrated in figure 4. Figure 4(a) shows the spectra without disturbance and figure 4(b) the spectra with the stimulated mode conversion. The frequency of the speaker and its higher harmonics are clearly visible in the spectra. The influence of this disturbance on the measured standard deviation increases with the core diameter of the fibres, as listed in table 2 But this correlation could also be a result of the unreproducible attachment to the speaker.

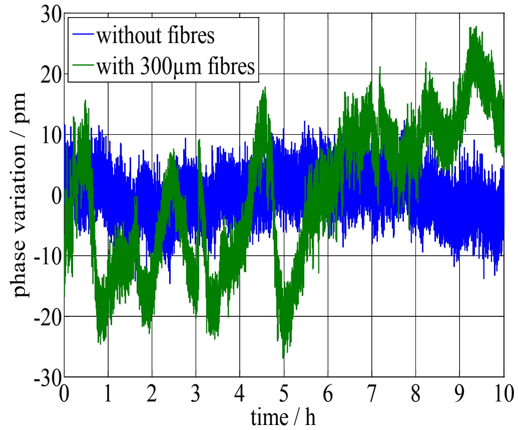

Figure 3: Phase variation measured at the Mach-Zehnder setup with and without 300 µm multimode fibres transferring the superposed beams over a time of 10 hours with an acquisition rate of 1 kHz

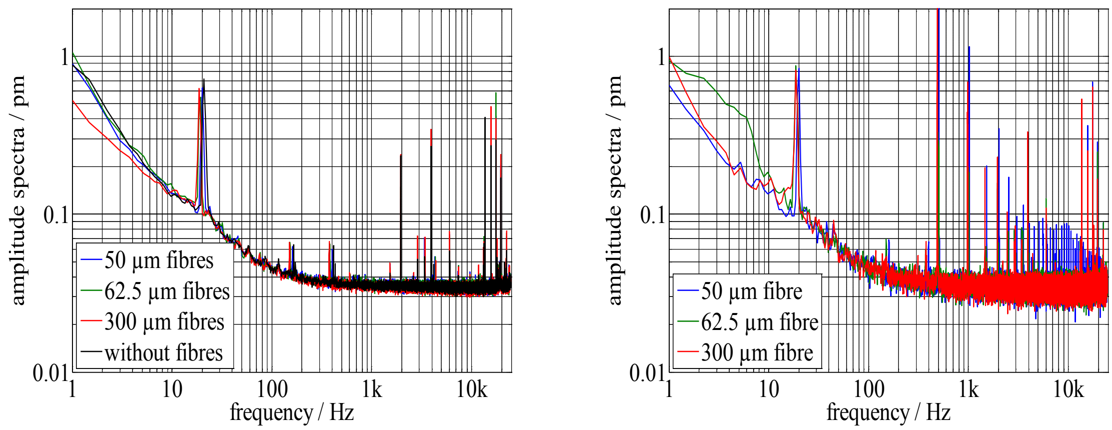

Figure 4(a): without disturbance

Figure 4(b): disturbance caused with speaker operating at 500 Hz

Figure 4: amplitude spectra of the phase variations at the Mach-Zehnder setup with multimode fibres to transfer the superposed beams to the detectors

5. DISCUSSION

The phase noise of a heterodyne interferometer was measured and calculated. It was shown, that an interferometer using a Prometheus laser as light source is shot and amplifier noise limited at a beat frequency of 4 MHz. But at a beat frequency of 1.5 MHz the relative intensity noise of the laser limits the resolution of the interferometer. This finding was verified using a Mach-Zehnder setup. A phase variation with a standard deviation of 4.8 pm was observed at a beat frequency of 4 MHz and a standard deviation of 11.3 pm at a beat frequency of 1.5 MHz. For a heterodyne interferometer with an aspired uncertainty in the sub-nanometre range the beat frequency has to be chosen with respect of the spectrum of the relative intensity noise of the light source.

The same phase variations which meant to be the resolution is achievable using multimode fibres at the interferometer output. It is necessary to separate heat sources to increase the stability of an interferometer setup. But a separation of the detectors using multimode fibres also reduces the long-time stability of the interferometer. Depending on the core diameter and the ambient conditions the phase variations introduced by the fibres may exceed the positive effects of the separation. This is especially true, if mode conversion is stimulated due to mechanical vibrations, temperature variations and variations of bending radius. Whether the measured disturbances disappear or not if singlemode fibres are used to guide the superposed beams will be part of further investigations.

REFERENCES

[1] P. Köchert, J. Flügge, C. Weichert, R. Köning and E. Manske, "Phase measurement of various commercial heterodyne He–Ne-laser interferometers with stability in the picometer regime", Measurement Science and Technology, 23, 074005, 2012

[2] C.-M. Wu, J. Lawall and R. D. Deslattes, "Heterodyne Interferometer with Subatomic Periodic Nonlinearity", Applied Optics, OSA, 38, 4089-4094, 1999

[3] C. Weichert, P. Köchert, R. Köning, J. Flügge, B. Andreas, U. Kuetgens and A. Yacoot, "A heterodyne interferometer with periodic nonlinearities smaller than ±10pm", Measurement Science and Technology, 2012, 23, 094005

[4] C. Weichert, J. Flügge, P. Köchert, R. Köning, and R. Tutsch, "Stability of a fiber-fed heterodyne interferometer", 10th IMEKO Symp. Laser Metrology for Precision Measurement and Inspection in Industry, vol. 2156 (Düsseldorf: VDI), pp 243–50, 2011

[5] S. Hosoe, "Highly precise and stable displacement-measuring laser interferometer with differential optical paths", Precision Engineering, 17, 258 – 265, 1995

[6] C. Weichert, J. Flügge, R. Köning, H. Bosse, and R. Tutsch, "Aspects on design and characterization of a high resolution heterodyne interferometer", Fringe 2009: Proc. 6th Int. Workshop on Advanced Optical Metrology, 263–268, 2009

[7] E. Massa, G. Mana, J. Krempel, M. and Jentschel, "Polarization delivery in heterodyne Interferometry", Opt. Express, OSA, 21, 27119-27126, 2013

[8] G. Cavagnero, G. Mana, and E. Massa, "Effect of recycled light in two-beam interferometry", Review of Scientific Instruments, 76, 053106-1 - 053106-6, 2005

[9] Joint Committee for Guides in Metrology JCGM Working Group 1, "Evaluation of measurement data — Guide to the expression of uncertainty in measurement", Bureau International des Poids et Measure, 2008

[10] V. Leonard, Coherent, private communication, 2013

[11] H. G. Unger, "Optische Nachrichtentechnik", Hüthig Verlag, Heidelberg, 1984

CONTACTS

Christoph Weichert	christoph.weichert@ptb.de
Paul Köchert	paul.koechert@ptb.de
Rainer Köning	rainer.koening@ptb.de
Jens Flügge	jens.fluegge@ptb.de